# Pre- and Postoperative Imaging of Knee Articular Cartilage

13

Avneesh B. Chhabra, Gaurav K. Thawait, and Gustav Andreisek

## 13.1 Introduction

Adult articular cartilage is avascular resulting in limited transport of inflammatory mediators and cells to the injured site; thus, cartilage damaged by trauma or degeneration has no intrinsic capacity to heal itself [1, 2]. Chondral injury, a frequent cause of pain and knee function limitation, poses a serious problem for orthopedic surgeons. The associated pain and physical disability can restrict an individual's ability to perform activities of daily living, which, in athletes, can even have career-ending consequences. Further, in the young population, cartilage lesions predispose to the development of precocious osteoarthritis.

Cartilage repair surgery is a highly dynamic research field. Over the past two decades, there have been several exciting, sophisticated surgical repair procedures for the treatment of focal traumatic or degenerative cartilage lesions, which in turn has created the need for an accurate, noninvasive assessment of the repair tissue. With its excellent soft tissue contrast and precise morphological evaluation of articular cartilage and repair tissue, magnetic resonance imaging (MRI) is the method of choice as a noninvasive and objective outcome measure [3–13].

Within the past decade, evolution of MRI technology has significantly improved the image quality. The cartilage-specific pulse sequences have enhanced the ability of qualitative (morphological) and quantitative (biochemical/functional) assessment of cartilage injury and repair. Higher magnetic field strengths have substantially increased the signal-to-noise ratio, spatial resolution, and speed of image acquisition; however, limitations to the increased field strength include greater amount of noise, imaging contrast issues, and safety concerns.

A. B. Chhabra, MBBS, MD (✉)
Department of Radiology and Orthopedic Surgery, University of Texas Southwestern Medical Center, Dallas, TX, USA

Department of Musculoskeletal Radiology, Parkland Health and Hospital System, Dallas, TX, USA
e-mail: avneesh.chhabra@utsouthwestern.edu

G. K. Thawait, MBBS, MD
Russell H. Morgan Department of Radiology and Radiological Science, Johns Hopkins University, Baltimore, MD, USA

Department of Biomedical Engineering, Johns Hopkins University, Baltimore, MD, USA

G. Andreisek, MD, MBA
Department of Radiology, University Hospital Zurich, University of Zurich, Zurich, Switzerland

Swiss Center for Musculoskeletal Imaging, Balgrist Campus AG, Zurich, Switzerland

Department of Radiology, St Claraspital, Basel, Switzerland

Department of Radiology, Spital Thurgau AG, Cantonal Hospital, Munsterlingen, Switzerland
e-mail: gustav@andreisek.de


H. K. Gahunia et al. (eds.), *Articular Cartilage of the Knee*,
https://doi.org/10.1007/978-1-4939-7587-7_13

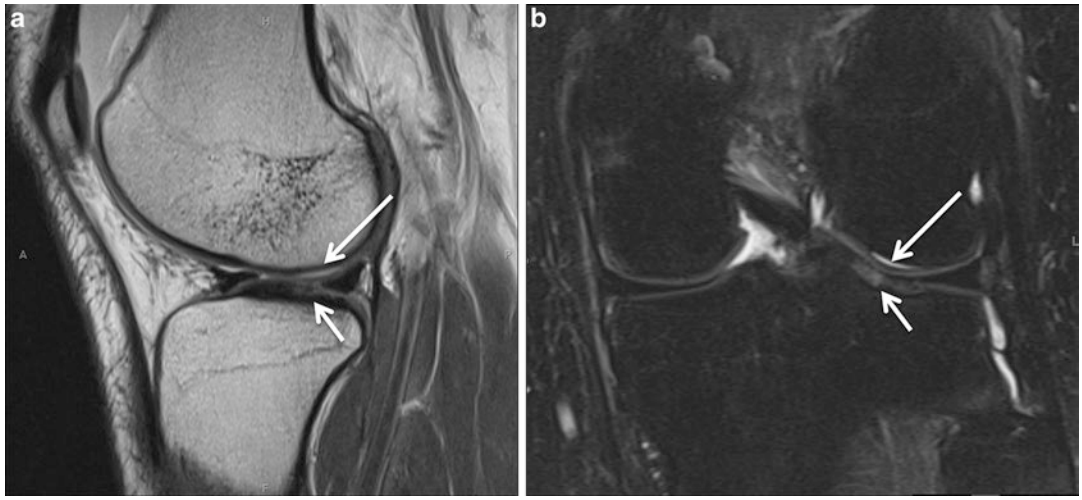


**Fig. 13.1** Sagittal proton density (**a**) and coronal fat-saturated proton density (**b**) MR images in a 33-year-old woman with knee pain. Note a focal area of articular cartilage delamination (large arrow) over the lateral femoral condyle and an irregular partial-thickness defect on the corresponding tibial surface (small arrows)

MR imaging of the knee is the method of choice to identify articular cartilage injuries and disease progression [14–17]. In order to evaluate the effectiveness or compare various therapeutic intervention and surgical treatments for chondral repair, an appropriate, reliable, and objective cartilage repair assessment system or combination of systems is necessary. MR imaging has been shown to be a reliable tool in the preoperative diagnosis of cartilage injury and postoperative evaluation of cartilage repair tissue [18–22]. During the postsurgical follow-up, MR imaging aids in assessing the surgical success or potential complications of cartilage repair procedures. In contrast to arthroscopy, MR imaging can assess the morphology, width, and depth of the repair tissue and evaluate the subchondral bone, as well as other internal derangements noninvasively. Although various biochemical techniques, such as T2 mapping, post-contrast T1 mapping, T1rho imaging, and sodium MR, enable the assessment of cartilage architecture, conventional anatomic and morphologic imaging remain the mainstay for pre- and postoperative assessment of the articular cartilage (Fig. 13.1).

In this chapter, we describe the role of MRI in the preoperative diagnosis of knee cartilage injury and postoperative follow-up as it relates to the visualization, assessment, and characterization of cartilage repair tissue. The cartilage repair tissue-specific MR techniques and the morphological/biochemical outcome of a given cartilage repair treatment procedure are reviewed in Chap. 14, whereas this chapter briefly summarizes the routinely used techniques and their advantages; provides an overview of the available treatment options, including their indications, technique, and clinical results; and illustrates the MR morphology of repair sites as well as postoperative complications. Further, we also discuss the two-dimensional (2D) and three-dimensional (3D) Magnetic Resonance Observation of Cartilage Repair Tissue (MOCART) scoring system, which has been well validated in studies of cartilage regeneration techniques.

## 13.2 Preoperative Assessment of Articular Cartilage Injury

Articular cartilage contributes to a large component of the load-bearing capability of the joint that is subjected to repetitive mechanical forces. In the event of an abnormal mechanical load or high impaction force, there may be focal carti-

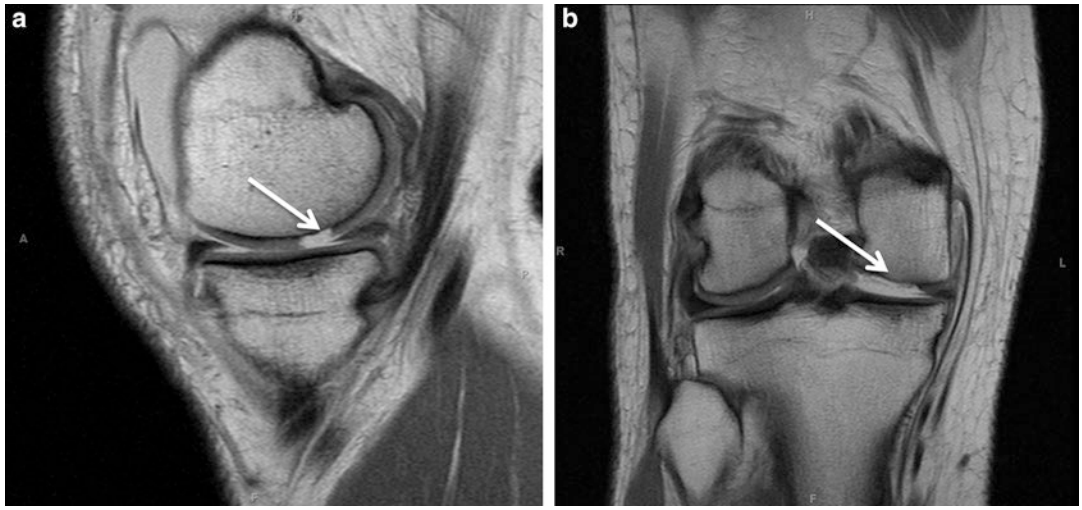


**Fig. 13.2** Sagittal (**a**) and coronal (**b**) proton density MR images of a 51-year-old man with recent knee injury. An area with shouldered cartilage defect over the medial femoral condyle can be seen (arrows)

lage injury. The acute trauma-related defect is usually focal and isolated and shows a shouldered margin (Fig. 13.2). The knowledge of such a defect, especially in young patient, is particularly important because articular cartilage has a limited capacity for spontaneous repair. Cartilage loss can further result in stress changes in the underlying bone, causing pain and decreased range of motion in the affected joint. Finally, cartilage injury can lead to premature joint degeneration in young adults leading to significant morbidity. A normal adult loses 1–3% of knee articular cartilage with aging, which further worsens with onset of osteoarthritis. The arthritis-related defects show irregular and obtuse margins due to repetitive wear and tear.

### 13.2.1 Role of Magnetic Resonance Imaging

The direct visualization of articular cartilage, multiplanar capabilities, and high soft tissue contrast provided by MRI enables the accurate and reproducible assessment of the morphologic features of injured articular cartilage. By using a cartilage-sensitive MR sequence, the adjacent joint fluid and subchondral bone can be distinguished from cartilage MR signal characteristics. The most commonly used clinical MR imaging techniques to assess the status of articular cartilage are fat-suppressed T2-weighted (fs T2W) or proton density-weighted (PDW) sequences. These MR images delineate the intermediate signal intensity of articular cartilage from the high signal intensity of joint fluid (Figs. 13.1 and 13.2). These images are also useful for accurate grading of the cartilage loss (low- or high-grade) and full-thickness defects, as well as for the detection of subchondral bone marrow edema and cyst formation, which shows increased signal intensity [23–25]. Fat-suppressed 3D sequences, such as fast spin echo (FSE) or spoiled gradient-recalled (SPGR) sequences and double-echo steady-state (DESS) sequences, provide excellent morphological depiction of the cartilage in multiple planes, thus, avoiding partial volume effects [26–29]. Higher spatial resolution and accuracy for individual cartilage lesions have been shown using 3D over 2D sequences in knee joint [30] and other smaller joints in accordance with the author's experience (Fig. 13.3). However, 3D gradient data sets are often more susceptible to metal artifacts and may be less sensitive to meniscal and ligament pathologies as well as subchondral bone marrow edema.

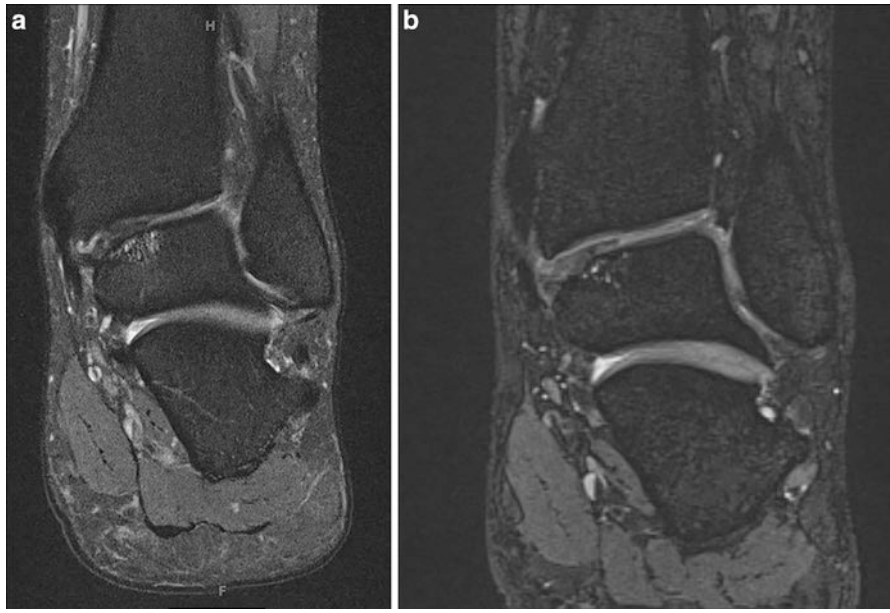


**Fig. 13.3** Coronal fat-saturated proton density (**a**) and coronal DESS (**b**) MR images of a 25-year-old woman with osteochondral lesion of the posteromedial talar dome. Note better depiction of bone marrow edema and cystic changes on fat-saturated proton density; however, the cartilage evaluation is limited on 2D sequence due to partial volume artifacts. Corresponding DESS imaging shows better cartilage demarcation and separates the tibial and talar articular cartilages

## 13.2.2 Treatment of Injured Articular Cartilage

Cartilage repair and regeneration is a treatment recommended for patients with knee cartilage damage or deterioration caused by:

- Injury or trauma, including sports injuries
- Repetitive use of the joint
- Congenital abnormalities affecting normal joint structure
- Hormonal disorders that affect bone and joint development, such as osteochondritis dissecans (OCD)

To determine the best cartilage repair approach for the patient, MRI is used to determine the severity, size, and location of cartilage injuries. The commonly used surgical techniques for the treatment of injured cartilage can be prudently classified into repair, reconstruction, and regeneration techniques [31]. For details of surgical procedure, refer to Chap. 11.

### 13.2.2.1 Repair Techniques

The simplest treatment for displaced, multifragmented, avascular, or deformed chondral lesions is removal of the lesion and debridement of its bony base. The principal indication for such an arthroscopic debridement is during the treatment of concurrent meniscal tears in patients with minimal malalignment [32]. Microfracture is a related older technique for the treatment of chondral lesions. Multiple perforations are arthroscopically created using an angulated ice pick crossing the subchondral bone to induce bleeding in the damaged site. Bleeding, which gradually creates a clot, brings various bone marrow elements including progenitor cells, cytokines, and growth factors that have the ability to form repair tissue. The hematopoietic and mesenchymal stem cells are stimulated to form the fibrocartilage composed of collagen types I and II, which is of inferior quality and not as resilient in dealing with stress when compared to the native articular cartilage. Microfractures are effective in small injuries/areas of cartilage

defects (less than 2 $cm^2$) with an intact subchondral plate [33, 34].

#### 13.2.2.2 Reconstruction Techniques

Osteochondral autograft transplantation (OAT) provides a structure that integrates well with the surrounding bone. An osteochondral (OC) graft is taken from a non-weight-bearing area of the knee and is transplanted into the cartilage defect site. The OC grafts are press fitted into the defect and flushed with the adjacent native cartilage to provide good contact with the healthy tissue. This can be achieved by placing the plugs perpendicular to the articular surface. The area of coverage is limited with a single OAT procedure. Alternatively, mosaicplasty is a procedure where multiple OC autografts cover a larger area.

Allografts are more adaptable and can be designed for any defect shape or size. The main limitations of this technique include risk of immune reaction and transmission of disease. Additionally, these allografts have to be used within a short period of time because of reduction in cell viability with time [35]. Allografts are indicated in young active patients with injuries greater than 2.5 cm in diameter [36].

Bioabsorbable devices have gained popularity because of the technical ease to arthroscopically implant them without the risk of blood-borne disease transmission or the requirement for removal of the implanted device. Also, the appropriate dimensions (thickness and length) can be chosen to fit the entire articular cartilage lesion.

#### 13.2.2.3 Regeneration Techniques

Autologous chondrocyte implantation (ACI) is a two-step technique that involves harvesting the articular cartilage from a non-weight-bearing area of the knee. The harvested chondrocytes are cultured to increase the chondrocyte count to two to five million cells, which are then reimplanted in the host knee cartilage defect site with an overlying periosteal patch. The main indication for this technique is failure of other techniques in patients less than 50 years of age with cartilage lesions between 1 and 10 $cm^2$ [15, 37]. The second- and third-generation ACI techniques have been subsequently developed to include the use of seeded membranes and biomaterials such as collagen type I or the chondro-inductive/chondro-conductive matrices. However, the comparison of first and second generation of ACI has not shown any significant clinical differences [38, 39].

## 13.3 Postoperative Assessment of Articular Cartilage Repair

MRI is used for the assessment of graft incorporation, graft congruity, and examination of the repair tissue characteristics. Postsurgical MRI is used for follow-up of patients after cartilage repair surgery in order to determine the success of surgical treatment and to assess the morphology and composition of the repair tissue. In the first 4 weeks after the procedure, the plugs and surrounding marrow have altered marrow signal. By 12 months, the plugs and the surrounding marrow return to normal fatty marrow signal. Persistent edema visualized as high signal intensity in the subchondral bone marrow and cyst formation indicates graft failure and poor incorporation.

### 13.3.1 Morphological Assessment of Articular Cartilage Repair: Qualitative

To successfully assess the graft morphology and integration to native tissue, it is essential to obtain a high spatial resolution, which in turn can be achieved either by using a surface coil (at 1.5 T scanner) or a knee coil (at 3 T scanner) [40–42]. Cartilage-sensitive MR sequences that allow excellent visualization of the articular cartilage with good signal-to-noise ratio (SNR) and contrast-to-noise ratio (CNR) within reasonable imaging times includes: fs PDW, T2 FSE and 3D gradient recalled echo (GRE) sequences [24, 30, 43–45]. Using a combination of these morphologic imaging sequences has provided excellent soft tissue contrast.

Several proposals for the morphological analysis of the repair tissue include evaluations of the structure and MR signal intensity of the repair

tissue (at its surface, the defect filling and integration with adjacent native cartilage); degree of defect filling; morphology of repair tissue with respect to native cartilage (flush, proud, or depressed); delamination (in the setting of ACI); integration with the adjacent native cartilage; nature of the interface with the adjacent surface (presence or absence and size of fissures); integrity of cartilage on the opposite articular surface; as well as the assessment of the status of the subchondral bone and bone marrow [40, 42, 46, 47].

#### 13.3.1.1 Two-Dimensional Magnetic Resonance Observation of Cartilage Repair Tissue Score

Among various MR scoring systems, the MOCART proposed by Marlovits et al. [40] is an efficient scoring system that has shown to have proven validity, reliability, and clinical usefulness with excellent interobserver reproducibility [40, 48, 49]. The MR assessment of the MOCART score is based on standard 2D MR sequences. Depending on the anatomic site of the cartilage repair, the MR evaluation of the cartilage repair tissue is performed on sagittal, axial, or coronal 2D planes using high spatial resolution together with a slice thickness of 2–4 mm. See Appendix C for details of 2D MOCART assessment criteria.

The 2D MOCART scoring system involved the analysis of the following nine variables:

1. Degree of defect repair and filling
2. Integration of cartilage repair tissue to border zone
3. Structure of repair tissue on surface
4. Structure of whole volume of repair tissue
5. Signal intensity of repair tissue
6. Constitution to subchondral lamina
7. Status of the subchondral bone
8. Possible adhesions
9. Possible joint effusion (Fig. 13.4)

#### 13.3.1.2 Three-Dimensional Magnetic Resonance Observation of Cartilage Repair Tissue Score

With improvement of MR technology, pulse sequences, and development of 3D sequences, Welsch et al. proposed a new 3D MOCART score by using the isotropic 3D TrueFISP sequence and its multiplanar reconstruction (MPR) [49]. The new isovoxel 3D sequences have the potential for high-resolution isotropic imaging with a voxel size down to 0.4 $mm^3$, which can then be reformatted in arbitrary planes without any loss of spatial resolution. Building on the capabilities of MPR, the cartilage repair 3D visualization and subsequent development of the 3D MOCART scoring system were feasible.

The 3D MOCART score was based on the standard 2D MOCART score by including variables and subcategories. The 3D MOCART included 11 variables as follows (see Appendix C for details of 3D MOCART assessment criteria):

1. Defect fill relative to adjacent native articular cartilage
2. Repair tissue interface with native cartilage
3. Bone interface
4. Surface of repair tissue
5. Structure of repair tissue
6. Signal intensity of repair tissue
7. Subchondral lamina
8. Chondral osteophyte
9. Bone marrow edema
10. Subchondral bone integrity
11. Effusion (Figs. 13.5 and 13.6)

A pertinent discussion of the variables in 3D MOCART score is as follows:

1. *Defect Fill*

   Defect fill is evaluated in comparison to the adjacent native cartilage. Defect fill is described as 100% (flush with the native cartilage), when the repair tissue is of comparable thickness to the adjacent cartilage. If


**Fig. 13.4** Coronal (**a**) and sagittal (**b**) fat-saturated proton density MR images of a 47-year-old woman with history of right knee pain. She had a prior lateral meniscectomy as well as microfracture surgery within the medial femoral condyle (arrows). 2D MOCART (Magnetic Resonance Observation of Cartilage Repair Tissue) staging for medial femoral condyle: (1) degree of defect repair and filling: complete (at the level of the adjacent cartilage); (2) integration to the border zone, complete (complete integration with adjacent cartilage) demarcating border visible, no; (3) surface of the repair tissue, surface intact; (4) structure of the repair tissue, fairly homogenous; (5) signal intensity of the repair tissue, dual T2-FSE isointense; (6) constitution to subchondral lamina, good; (7) subchondral bone, subchondral cysts and bone marrow edema; (8) adhesions, no; (9) joint effusion, yes. After a 2-year follow-up, sagittal (**c**) and coronal (**d**) fat-saturated proton density MR show decreased bone marrow edema and cystic changes on medial femoral condyle (large arrows). However, coronal image also shows worsening lateral compartment cartilage loss with developing bone marrow edema (small arrow)

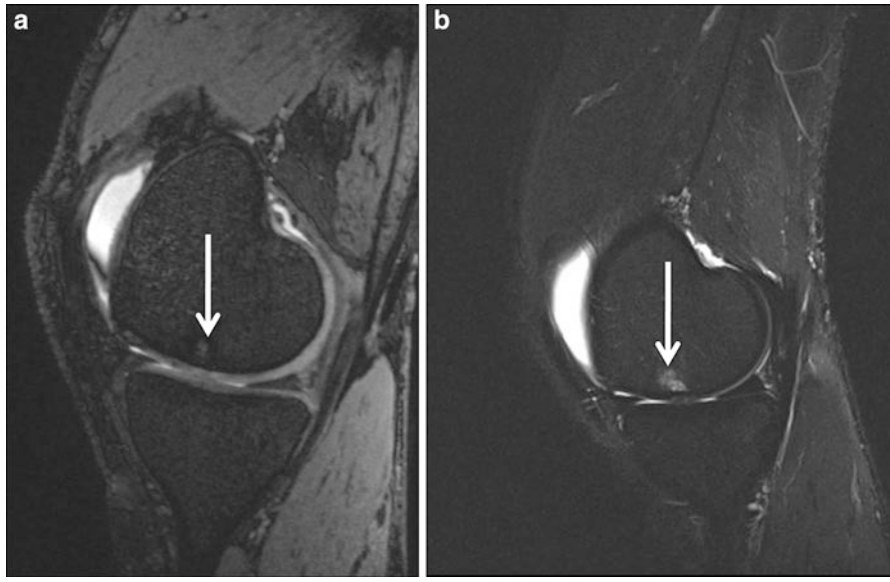


**Fig. 13.5** Sagittal 3D DESS (**a**) and sagittal fat-saturated proton density (**b**) MR images of a 47-year-old woman with a prior microfracture surgery within the medial femoral condyle (arrows). Notice better depiction of cartilage definition on 3D image (**a**) and reactive bone marrow changes in the medial femoral condyle on 2D image (**b**), respectively

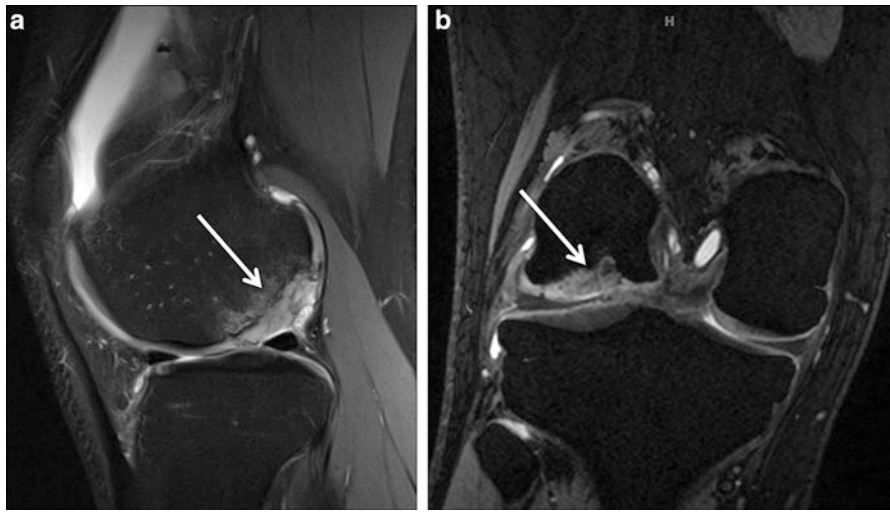


**Fig. 13.6** Sagittal fat-saturated proton density (**a**) and coronal (**b**) 3D TrueFISP MR images of a 15-year-old boy with history of prior ACI within the lateral femoral condyle (arrows). 3D MOCART (Magnetic Resonance Observation of Cartilage Repair Tissue) staging for medial femoral condyle: (1) degree of defect repair and filling, complete and hypertrophy (75–100% above the level of the adjacent cartilage); (2) cartilage interface (integration to the border zone), complete; (3) surface of the repair tissue, surface irregular; (4) structure of the whole repair tissue, fairly homogeneous; (5) signal intensity, dual T2-FSE isointense; 3D TrueFISP, isointense; (6) constitution to subchondral lamina, good; (7) subchondral lamina, irregular; (8) chondral osteophyte, no; (9) bone marrow edema, yes, medium; (10) subchondral bone, cysts; joint effusion, yes, medium

the value is below 100%, it is referred to as a cartilage defect underfilling, and if it is above 100% (proud relative to the native cartilage), it is termed as hypertrophy. Further, it can be classified on the basis of localization in the weight-bearing areas or elsewhere.

2. *Cartilage Interface*

   It refers to the integration of the repair tissue to the native cartilage border zone. It is stated as complete or incomplete, depending upon the presence or absence of gap at the interface between the repair tissue and the adjacent cartilage.

3. *Bone Interface*

   This evaluates integration of the repair tissue to the subchondral bone or the integration to a possible periosteal flap depending on surgical technique. It is reported as completely attached, partially detached, or complete detached.

4. *Repair Tissue Surface*

   The cartilage surface may be damaged with the appearance of fibrillations, fissures, or ulcerations above or below 50% of repair tissue depth, or there may be a total degeneration. Further, any signs of adhesions are also recorded at the site of damage.

5. *Repair Tissue Structure*

   The architecture of the repaired cartilage is reported as homogeneous when there is typical cartilage layering over the entire repair tissue or inhomogeneous if it shows cleft formation.

6. *MR Signal Intensity*

   The signal intensity of the repair tissue is compared to the adjacent native cartilage. It can be evaluated as nearly normal or abnormal, depending on the amount of the signal alterations. The abnormal signal intensity can be higher (hyperintense) or lower (hypointense) relative to native articular cartilage.

7. *Subchondral Lamina*

   The subchondral lamina between the repair tissue and the bone is reported as either intact or irregular and broken.

8. *Chondral Osteophyte*

   Osteophytes can emerge in the region of the cartilage transplant. Further, they can be found in different sizes, which can be classified based on their thickness of above or below 50% of the thickness of the cartilage transplant.

9. *Bone Marrow Edema*

   Subchondral bone marrow edema size can be classified as small (diameter, < 1 cm), medium (< 2 cm), large (< 4 cm), or diffuse.

10. *Subchondral Bone*

    Excluding the bone marrow edema, the subchondral bone criteria evaluate the changes in the subchondral bone adjacent to the area of repair tissue such as the presence of granulation tissue, sclerosis, or cysts.

11. *Effusion*

    Based on the extent, joint effusion is classified as absent, small, medium, or large.

In the clinical routine follow-up after cartilage repair, the 2D evaluation with the standard 2D MOCART scoring system obtained by using three standard MR sequences provided comparable information to the 3D MOCART scoring system assessed by using only one high-resolution isotropic 3D TrueFISP sequence. However, artifacts were more frequently visible within the 3D TrueFISP sequence.

Another MRI scoring system, the cartilage repair osteoarthritis knee score (CROAKS) was developed for follow-up of knee cartilage repair procedures integrating assessment of the repair site and the whole joint [50]. This semiquantitative assessment system combined the assessment of the cartilage repair site using features of MOCART scores and for the whole the joint based on experiences with the Magnetic Resonance Imaging Osteoarthritis Knee Score (MOAKS). MRI examinations of 20 patients at 12 months post matrix-associated autologous chondrocyte transplantation (MACT) of the knee showed good to excellent reliability with the combined, established semiquantitative scoring systems (MOCART and MOAKS) [50].

### 13.3.2 Magnetic Resonance Imaging Assessment of Repair Tissue

Recently, there has been a great interest in developing MR imaging techniques to evaluate the biochemical composition of the cartilage repair procedure. The proteoglycan content MR specific sequences include delayed gadolinium-enhanced MR imaging of cartilage (dGEMRIC), T1rho mapping, and sodium MR imaging, whereas the collagen content-sensitive techniques include T2 mapping and magnetization transfer [51–53].

Chondrocytes usually repair by formation of fibrocartilage composed of collagen types I and II, which is not as resilient in dealing with stress as the compressive, native hyaline cartilage primarily composed of collagen type II. On MR imaging, initially the tissue may be indistinct; however, by 1–2 years, repair tissue is expected to fill the defect with a smooth contour. The signal intensity may be similar, although more commonly, less than the native cartilage related to predominant fibrocartilage formation [14]. Following surgical treatment, underlying bone marrow edema often regresses but may not resolve completely. Surface fissures and flaps may be present (Fig. 13.7).

MRI has been proven to be highly accurate in assessing the repair tissue with good correlation to the lesion fill and tissue quality and its integration with the adjacent native cartilage [54]. Further, at post-surgery and during follow-up, MR imaging facilitates accurate assessment of complications of repair surgery including graft/periosteal hypertrophy and delamination, adhesions, surface incongruence, and reactive/inflammatory changes (such as effusions and synovitis). Based on the treatment procedure, the nature of the repair tissue is outlined below:

#### 13.3.2.1 Abrasion Arthroplasty/ Debridement

Removal of few millimeters of subchondral bone causes local bleeding, fibrin clot formation, and subsequent development of a fibrocartilage-like tissue composed of collagen type I and type III. Fibrocartilage is stronger against tension rather than compression forces and is therefore not a durable long-lasting substitute for hyaline cartilage. Although early results and symptom relief from this procedure were promising, long-term results have not been satisfactory [55].

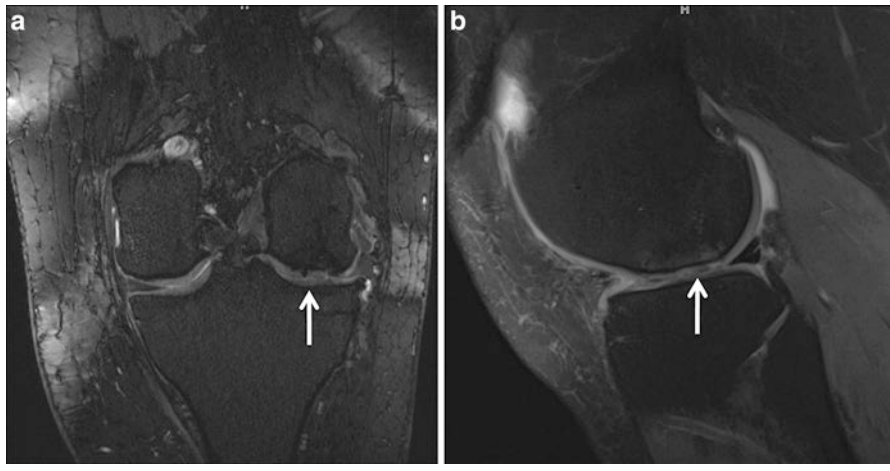


**Fig. 13.7** Coronal 3D DESS (**a**) and sagittal fat-saturated proton density (**b**) MR images of a young woman with a prior microfracture surgery within the lateral femoral condyle (arrows). Notice good cartilage fill and better depiction of cartilage definition on the 3D image (**a**) with minimal surface irregularities

#### 13.3.2.2 Autologous Osteochondral Grafts

The repaired tissue is better when OAT is used in the femoral condyles rather than in the tibial plateau or in the patella [56]. The problems of lack of integration or fibrocartilage formation at the border zone with native cartilage may occur. MRI after the mosaicplasty procedure involves assessment of graft incorporation, graft congruity, and examination of the repair tissue characteristics. In the first 4 weeks after the procedure, the plugs and surrounding marrow have altered marrow signal. By 12 months, the plugs and the surrounding marrow return to normal fatty marrow signal. Persistent edema like subchondral bone marrow signal and cyst formation indicates graft failure and poor incorporation.

#### 13.3.2.3 Allogenic Osteochondral Transplants

MRI is useful in determining the surface congruity between graft and the native cartilage [14]. Usually, the bony plug margin is also visible indicating the type of repair. Bone marrow edema can be prominent for up to 12 months post-surgery. Graft-host reactions can be seen as persistent signal abnormalities within the graft marrow or at the graft-host interface [57].

#### 13.3.2.4 Synthetic Grafts, Scaffolds, and Osteochondral Plugs

The synthetic plugs are radiolucent but can be visualized on MR imaging with varying signal intensity depending on the biomaterial used. Frequently, during the first few months, these plugs appear as low signal intensity tracts on T1W and T2W MR images. However, by the end of the first year, the grafts with repair tissue become hyperintense on T2W MR images. Most of them are not visible after 2 years [58].

#### 13.3.2.5 Autologous Chondrocyte Implants

During the follow-up of post ACI cartilage repair, MRI can accurately detect and classify the defect fill as flush, underfilling, or hypertrophy as well as the graft integration [59]. Surface irregularity is commonly seen on MR imaging (Fig. 13.6) [15]. The signal intensity of repair cartilage decreases after the first 12 months. Persistent bone marrow edema, chondral osteophytes, and cartilage delamination are adverse outcome indicative of ACI failure (Fig. 13.8). The common complications of ACI technique are symptomatic graft hypertrophy, perturbed fusion or integration, delamination, and fibrosis, which may require re-intervention [60–62]. Among

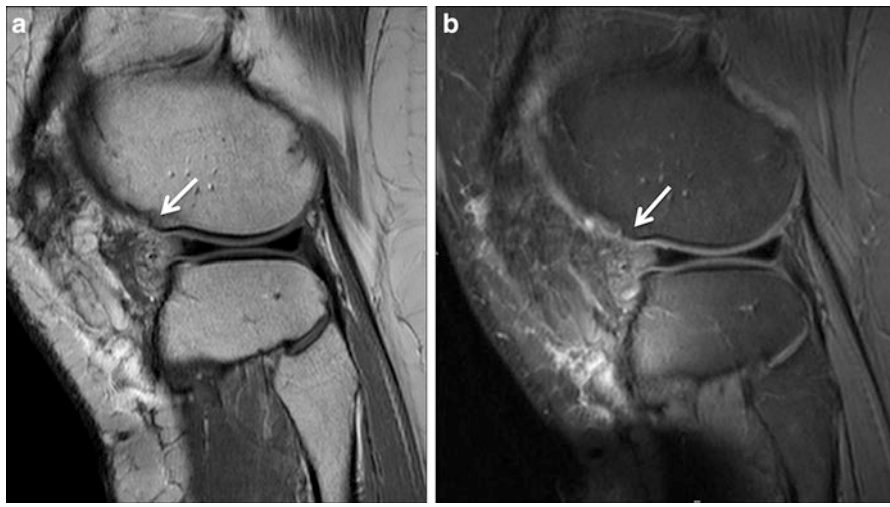


**Fig. 13.8** Sagittal proton density (**a**) and sagittal fat-saturated proton density (**b**) MR images of a young man with a prior ACI repair surgery within the lateral femoral condyle 1 year ago (arrows). Notice failure of ACI repair with visible chondral osteophytes (large arrow) and overlying cartilage delamination (small arrow)

those, the overall complication rate and incidence of hypertrophy of the transplant were higher for periosteum-covered ACI. Graft hypertrophy may occur 3–7 months post ACI and has been reported as a complication in 10–63% of cases [16–18]. Furthermore, an increased rate of symptomatic hypertrophy was found for patellar defects. Delamination occurs when the graft separates from the parent bone, which is visualized in MR as a linear fluid high signal intensity undermining the graft. When significant, both delamination and graft hypertrophy may require repeat surgery, either debridement in the case of hypertrophy or repeat ACI in both cases.

## 13.4 Conclusions

Cartilage injuries are common and a variety of repair procedures have been developed for their treatment. MR imaging has proven to be an excellent tool for presurgical mapping and postsurgical assessment of these lesions.

## References


1. Mankin HJ. The response of articular cartilage to mechanical injury. J Bone Joint Surg Am. 1982;64(3):460–6. Epub 1982/03/01.
2. Newman AP. Articular cartilage repair. Am J Sports Med. 1998;26(2):309–24. Epub 1998/04/21.
3. Ebert JR, Fallon M, Ackland TR, Janes GC, Wood DJ. Minimum 10-year clinical and radiological outcomes of a randomized controlled trial evaluating 2 different approaches to full weight bearing after matrix-induced autologous chondrocyte implantation. Am J Sports Med. 2020;48(1):133–42.
4. Donoso R, Figueroa D, Espinoza J, Yañez C, Saavedra J. Osteochondral autologous transplantation for treating patellar high-grade chondral defects: a systematic review. Orthop J Sports Med. 2019;7(10):2325967119876618.
5. Zhao X, Ruan J, Tang H, Li J, Shi Y, et al. Multicompositional MRI evaluation of repair cartilage in knee osteoarthritis with treatment of allogeneic human adipose-derived mesenchymal progenitor cells. Stem Cell Res Ther. 2019;10(1):308.
6. Kyriakidis T, Iosifidis M, Michalopoulos E, Melas I, Stavropoulos-Giokas C, et al. Good mid-term outcomes after adipose-derived culture-expanded mesenchymal stem cells implantation in knee focal cartilage defects. Knee Surg Sports Traumatol Arthrosc. 2019. https://doi.org/10.1007/s00167-019-05688-9. [Epub ahead of print].
7. Schreiner MM, Raudner M, Marlovits S, Bohndorf K, Weber M, et al. The MOCART (Magnetic Resonance Observation of Cartilage Repair Tissue) 2.0 knee score and atlas. Cartilage. 2019:1947603519865308. https://doi.org/10.1177/1947603519865308. [Epub ahead of print].
8. Ackermann J, Mestriner AB, Shah N, Gomoll AH. Effect of autogenous bone marrow aspirate treatment on magnetic resonance imaging integration of osteochondral allografts in the knee: a matched comparative imaging analysis. Arthroscopy. 2019;35(8):2436–44.
9. Liu YW, Tran MD, Skalski MR, Patel DB, White EA, et al. MR imaging of cartilage repair surgery of the knee. Clin Imaging. 2019;58:129–39.
10. Ogura T, Merkely G, Bryant T, Winalski CS, Minas T. Autologous chondrocyte implantation "Segmental-sandwich" technique for deep osteochondral defects in the knee: clinical outcomes and correlation with magnetic resonance imaging findings. Orthop J Sports Med. 2019;7(5):2325967119847173.
11. Trattnig S, Raudner M, Schreiner M, Roemer F, Bohndorf K. Biochemical cartilage imaging-update 2019. Radiologe. 2019;59(8):742–9.
12. de Girolamo L, Schönhuber H, Viganò M, Bait C, Quaglia A, et al. Autologous Matrix-Induced Chondrogenesis (AMIC) and AMIC enhanced by autologous concentrated Bone Marrow Aspirate (BMAC) allow for stable clinical and functional improvements at up to 9 years follow-up: results from a randomized controlled study. J Clin Med. 2019;8(3). pii: E392. https://doi.org/10.3390/jcm8030392.
13. Kreuz PC, Kalkreuth RH, Niemeyer P, Uhl M, Erggelet C. Long-term clinical and MRI results of matrix-assisted autologous chondrocyte implantation for articular cartilage defects of the knee. Cartilage. 2019;10(3):305–13.
14. Alparslan L, Winalski CS, Boutin RD, Minas T. Postoperative magnetic resonance imaging of articular cartilage repair. Semin Musculoskelet Radiol. 2001;5(4):345–63.
15. Brittberg M, Winalski CS. Evaluation of cartilage injuries and repair. J Bone Joint Surg Am. 2003;85-A(Suppl 2):58–69.
16. Potter HG, Foo LF. Magnetic resonance imaging of articular cartilage: trauma, degeneration, and repair. Am J Sports Med. 2006;34(4):661–77.
17. Welsch GH, Mamisch TC, Hughes T, Domayer S, Marlovits S, Trattnig S. Advanced morphological and biochemical magnetic resonance imaging of cartilage repair procedures in the knee joint at 3 tesla. Semin Musculoskelet Radiol. 2008;12(3):196–211.
18. Disler DG. Fat-suppressed three-dimensional spoiled gradient-recalled MR imaging: assessment of articular and physeal hyaline cartilage. AJR Am J Roentgenol. 1997;169(4):1117–23.
19. Kawahara Y, Uetani M, Nakahara N, Doiguchi Y, Nishiguchi M, Futagawa S, et al. Fast spin-echo MR of the articular cartilage in the osteoarthrotic knee.

Correlation of MR and arthroscopic findings. Acta Radiol. 1998;39(2):120–5.
20. Yoshioka H, Stevens K, Hargreaves BA, Steines D, Genovese M, Dillingham MF, et al. Magnetic resonance imaging of articular cartilage of the knee: comparison between fat-suppressed three-dimensional SPGR imaging, fat-suppressed FSE imaging, and fat-suppressed three-dimensional DEFT imaging, and correlation with arthroscopy. J Magn Reson Imaging. 2004;20(5):857–64.
21. Hede K, Christensen BB, Jensen J, Foldager CB, Lind M. Combined bone marrow aspirate and platelet-rich plasma for cartilage repair: two-year clinical results. Cartilage. 2019:1947603519876329. https://doi.org/10.1177/1947603519876329. [Epub ahead of print].
22. Monckeberg JE, Rafols C, Apablaza F, Gerhard P, Rosales J. Intra-articular administration of peripheral blood stem cells with platelet-rich plasma regenerated articular cartilage and improved clinical outcomes for knee chondral lesions. Knee. 2019;26(4):824–31.
23. Bredella MA, Tirman PF, Peterfy CG, Zarlingo M, Feller JF, Bost FW, et al. Accuracy of T2-weighted fast spin-echo MR imaging with fat saturation in detecting cartilage defects in the knee: comparison with arthroscopy in 130 patients. AJR Am J Roentgenol. 1999;172(4):1073–80.
24. Potter HG, Linklater JM, Allen AA, Hannafin JA, Haas SB. Magnetic resonance imaging of articular cartilage in the knee. An evaluation with use of fast-spin-echo imaging. J Bone Joint Surg Am. 1998;80(9):1276–84.
25. Ebert JR, Smith A, Fallon M, Wood DJ, Ackland TR. Degree of preoperative subchondral bone edema is not associated with pain and graft outcomes after matrix-induced autologous chondrocyte implantation. Am J Sports Med. 2014;42(11):2689–98. Epub 2014/09/13.
26. Yang X, Li Z, Cao Y, Xu Y, Wang H, et al. Efficacy of magnetic resonance imaging with an SPGR sequence for the early evaluation of knee cartilage degeneration and the relationship between cartilage and other tissues. J Orthop Surg Res. 2019;14(1):152.
27. Chaudhari AS, Stevens KJ, Sveinsson B, Wood JP, Beaulieu CF, et al. Combined 5-minute double-echo in steady-state with separated echoes and 2-minute proton-density-weighted 2D FSE sequence for comprehensive whole-joint knee MRI assessment. J Magn Reson Imaging. 2019;49(7):e183–94.
28. Hayashi D, Roemer FW, Guermazi A. Magnetic resonance imaging assessment of knee osteoarthritis: current and developing new concepts and techniques. Clin Exp Rheumatol. 2019;37 Suppl 120(5):88–95.
29. Hayashi D, Li X, Murakami AM, Roemer FW, Trattnig S, et al. Understanding magnetic resonance imaging of knee cartilage repair: a focus on clinical relevance. Cartilage. 2018;9(3):223–36.
30. Disler DG, McCauley TR, Kelman CG, Fuchs MD, Ratner LM, Wirth CR, et al. Fat-suppressed three-dimensional spoiled gradient-echo MR imaging of hyaline cartilage defects in the knee: comparison with standard MR imaging and arthroscopy. AJR Am J Roentgenol. 1996;167(1):127–32.
31. Forriol F. Growth factors in cartilage and meniscus repair. Injury. 2009;40(Suppl 3):S12–6.
32. Merchan EC, Galindo E. Arthroscope-guided surgery versus nonoperative treatment for limited degenerative osteoarthritis of the femorotibial joint in patients over 50 years of age: a prospective comparative study. Arthroscopy. 1993;9(6):663–7.
33. Steadman JR, Miller BS, Karas SG, Schlegel TF, Briggs KK, Hawkins RJ. The microfracture technique in the treatment of full-thickness chondral lesions of the knee in National Football League players. J Knee Surg. 2003;16(2):83–6.
34. Steadman JR, Briggs KK, Rodrigo JJ, Kocher MS, Gill TJ, Rodkey WG. Outcomes of microfracture for traumatic chondral defects of the knee: average 11-year follow-up. Arthroscopy. 2003;19(5):477–84.
35. McGoveran BM, Pritzker KP, Shasha N, Price J, Gross AE. Long-term chondrocyte viability in a fresh osteochondral allograft. J Knee Surg 2002 Spring;15(2):97–100.
36. Gross AE, Kim W, Las Heras F, Backstein D, Safir O, Pritzker KP. Fresh osteochondral allografts for posttraumatic knee defects: long-term followup. Clin Orthop Relat Res. 2008;466(8):1863–70.
37. Vaquero J, Forriol F. Knee chondral injuries: clinical treatment strategies and experimental models. Injury. 2011;43:694–705.
38. Bartlett W, Skinner JA, Gooding CR, Carrington RW, Flanagan AM, Briggs TW, et al. Autologous chondrocyte implantation versus matrix-induced autologous chondrocyte implantation for osteochondral defects of the knee: a prospective, randomised study. J Bone Joint Surg Br. 2005;87(5):640–5.
39. Manfredini M, Zerbinati F, Gildone A, Faccini R. Autologous chondrocyte implantation: a comparison between an open periosteal-covered and an arthroscopic matrix-guided technique. Acta Orthop Belg. 2007;73(2):207–18.
40. Marlovits S, Striessnig G, Resinger CT, Aldrian SM, Vecsei V, Imhof H, et al. Definition of pertinent parameters for the evaluation of articular cartilage repair tissue with high-resolution magnetic resonance imaging. Eur J Radiol. 2004;52(3):310–9. Epub 2004/11/17.
41. Qian Y, Williams AA, Chu CR, Boada FE. High-resolution ultrashort echo time (UTE) imaging on human knee with AWSOS sequence at 3.0 T. J Magn Reson Imaging. 2012;35(1):204–10. Epub 2011/10/18.
42. Trattnig S, Millington SA, Szomolanyi P, Marlovits S. MR imaging of osteochondral grafts and autologous chondrocyte implantation. Eur Radiol. 2007;17(1):103–18. Epub 2006/06/28.
43. Recht M, White LM, Winalski CS, Miniaci A, Minas T, Parker RD. MR imaging of cartilage repair procedures. Skelet Radiol. 2003;32(4):185–200. Epub 2003/03/26.

44. Recht MP, Piraino DW, Paletta GA, Schils JP, Belhobek GH. Accuracy of fat-suppressed three-dimensional spoiled gradient-echo FLASH MR imaging in the detection of patellofemoral articular cartilage abnormalities. Radiology. 1996;198(1):209–12. Epub 1996/01/01.
45. Trattnig S, Mlynarik V, Huber M, Ba-Ssalamah A, Puig S, Imhof H. Magnetic resonance imaging of articular cartilage and evaluation of cartilage disease. Invest Radiol. 2000;35(10):595–601. Epub 2000/10/21.
46. Trattnig S, Ba-Ssalamah A, Pinker K, Plank C, Vecsei V, Marlovits S. Matrix-based autologous chondrocyte implantation for cartilage repair: noninvasive monitoring by high-resolution magnetic resonance imaging. Magn Reson Imaging. 2005;23(7):779–87. Epub 2005/10/11.
47. Roberts S, McCall IW, Darby AJ, Menage J, Evans H, Harrison PE, et al. Autologous chondrocyte implantation for cartilage repair: monitoring its success by magnetic resonance imaging and histology. Arthritis Res Ther. 2003;5(1):R60–73. Epub 2003/04/30.
48. van den Borne MP, Raijmakers NJ, Vanlauwe J, Victor J, de Jong SN, Bellemans J, et al. International Cartilage Repair Society (ICRS) and Oswestry macroscopic cartilage evaluation scores validated for use in Autologous Chondrocyte Implantation (ACI) and microfracture. Osteoarthritis Cartilage. 2007;15(12):1397–402.
49. Welsch GH, Zak L, Mamisch TC, Resinger C, Marlovits S, Trattnig S. Three-dimensional magnetic resonance observation of cartilage repair tissue (MOCART) score assessed with an isotropic three-dimensional true fast imaging with steady-state precession sequence at 3.0 tesla. Invest Radiol. 2009;44(9):603–12.
50. Roemer FW, Guermazi A, Trattnig S, Apprich S, Marlovits S, Niu J, et al. Whole joint MRI assessment of surgical cartilage repair of the knee: cartilage repair osteoarthritis knee score (CROAKS). Osteoarthritis Cartilage. 2014;22(6):779–99. Epub 2014/04/02.
51. Krusche-Mandl I, Schmitt B, Zak L, Apprich S, Aldrian S, Juras V, et al. Long-term results 8 years after autologous osteochondral transplantation: 7 T gagCEST and sodium magnetic resonance imaging with morphological and clinical correlation. Osteoarthritis Cartilage. 2012;20(5):357–63. Epub 2012/02/23.
52. Eshed I, Trattnig S, Sharon M, Arbel R, Nierenberg G, Konen E, et al. Assessment of cartilage repair after chondrocyte transplantation with a fibrin-hyaluronan matrix–correlation of morphological MRI, biochemical T2 mapping and clinical outcome. Eur J Radiol. 2012;81(6):1216–23. Epub 2011/04/05.
53. Collins AT, Hatcher CC, Kim SY, Ziemian SN, Spritzer CE, et al. Selective enzymatic digestion of proteoglycans and collagens alters cartilage T1rho and T2 relaxation times. Ann Biomed Eng. 2019;47(1):190–201.
54. Ramappa AJ, Gill TJ, Bradford CH, Ho CP, Steadman JR. Magnetic resonance imaging to assess knee cartilage repair tissue after microfracture of chondral defects. J Knee Surg. 2007;20(3):228–34.
55. Bert JM, Maschka K. The arthroscopic treatment of unicompartmental gonarthrosis: a five-year follow-up study of abrasion arthroplasty plus arthroscopic debridement and arthroscopic debridement alone. Arthroscopy. 1989;5(1):25–32.
56. Bentley G, Biant LC, Carrington RW, Akmal M, Goldberg A, Williams AM, et al. A prospective, randomised comparison of autologous chondrocyte implantation versus mosaicplasty for osteochondral defects in the knee. J Bone Joint Surg Br. 2003;85(2):223–30.
57. Sirlin CB, Brossmann J, Boutin RD, Pathria MN, Convery FR, Bugbee W, et al. Shell osteochondral allografts of the knee: comparison of mr imaging findings and immunologic responses. Radiology. 2001;219(1):35–43.
58. Furukawa T, Eyre DR, Koide S, Glimcher MJ. Biochemical studies on repair cartilage resurfacing experimental defects in the rabbit knee. J Bone Joint Surg Am. 1980;62(1):79–89.
59. Ho YY, Stanley AJ, Hui JH, Wang SC. Postoperative evaluation of the knee after autologous chondrocyte implantation: what radiologists need to know. Radiographics. 2007;27(1):207–20. discussion 221-2.
60. Brown WE, Potter HG, Marx RG, Wickiewicz TL, Warren RF. Magnetic resonance imaging appearance of cartilage repair in the knee. Clin Orthop Relat Res. 2004;422(422):214–23.
61. Henderson I, Gui J, Lavigne P. Autologous chondrocyte implantation: natural history of postimplantation periosteal hypertrophy and effects of repair-site debridement on outcome. Arthroscopy. 2006 Dec;22(12):1318–1324.e1.
62. Recht MP, Goodwin DW, Winalski CS, White LM. MRI of articular cartilage: revisiting current status and future directions. AJR Am J Roentgenol. 2005;185(4):899–914.